Generation and annihilation of boron–oxygen-related recombination centers in compensated *p*- and *n*-type silicon

Bianca Lim,[1,a)] Fiacre Rougieux,[2] Daniel Macdonald,[2] Karsten Bothe,[1] and Jan Schmidt[1]
[1]*Institute for Solar Energy Research Hamelin (ISFH), Am Ohrberg 1, D-31860 Emmerthal, Germany*
[2]*School of Engineering, College of Engineering and Computer Science, The Australian National University, Canberra ACT 0200, Australia*

(Received 9 August 2010; accepted 5 October 2010; published online 30 November 2010)

The impact of boron–oxygen-related recombination centers as well as their defect kinetics have been intensely studied in boron-doped oxygen-rich *p*-type crystalline silicon. Experimental data for the defect in simultaneously boron- and phosphorus-doped compensated *p*- and *n*-type silicon, however, is sparse. In this study, we present time-resolved carrier lifetime measurements on Czochralski-grown silicon (Cz-Si) doped with both boron and phosphorus under illumination at 30 °C (defect generation) as well as at 200 °C in the dark (defect annihilation). The defect generation in compensated *n*-type Cz-Si is found to proceed on a similar time scale as the defect generation in (compensated) *p*-type Cz-Si. However, the shape of the carrier lifetime reduction during defect generation in compensated *n*-type silicon differs considerably from that in (compensated) *p*-type Cz-Si. The defect annihilation in compensated *n*-type Cz-Si is found to take up to 1000 times longer than in (compensated) *p*-type Cz-Si. In addition, we confirm a linear dependence of the normalized defect concentration N_t^* on the net doping concentration p_0 as well as a proportionality between the defect generation rate R_{gen} and the square of the net doping concentration p_0^2 in compensated *p*-type Cz-Si. These results cannot be explained by the established B_sO_{2i} defect model, however, they agree with a recently proposed defect model in which the defect is composed of one interstitial boron atom and an interstitial oxygen dimer (B_iO_{2i}).
 [doi:10.1063/1.3511741]

I. INTRODUCTION

Light-induced degradation (LID) of the carrier lifetime in oxygen-rich boron-doped crystalline silicon due to the formation of boron–oxygen-related recombination centers is a well-known and intensely studied phenomenon.[1–6] In B-doped Czochralski-grown silicon (Cz-Si) with sufficiently low metal concentrations, the boron–oxygen-related defect has been found to ultimately limit the carrier lifetime.[5] As a consequence, this defect also plays an important role for solar cells fabricated on such material, since it limits the open-circuit voltage and accordingly the energy conversion efficiency. The recombination center can be annihilated by a short anneal in the dark, leading to a recovery of the carrier lifetime.[1,2] However, subsequent illumination results in renewed generation of the defect and accordingly in renewed degradation of the lifetime.

While most of the previous work has focused on (exclusively) boron-doped *p*-type silicon, LID has also been observed in B-doped *n*-type silicon, which was overcompensated through the formation of thermal donors.[7] Very recently, LID was observed in *n*-type Cz-Si, which was doped with both boron and phosphorus.[8] However, no detailed time dependencies of either the defect generation or its annihilation were reported.

In this work, we present time-resolved studies of both defect generation under illumination and defect annihilation in the dark at 200 °C in boron- and phosphorus-doped *p*- and *n*-type Cz-Si with varying net doping concentrations p_0 and n_0, respectively. While the defect generation is found to proceed in similar time intervals in compensated *p*- and *n*-type Cz-Si, the evolution of the lifetime during defect generation differs considerably in both cases. The defect annihilation is found to take significantly longer in *n*-type silicon when compared to *p*-type silicon of similar net doping. In addition, we confirm recent reports that the normalized defect concentration N_t^* increases linearly with the net doping concentration p_0 and present data which supports recent findings that the defect generation rate R_{gen} in compensated *p*-type Cz-Si scales with the square of the net doping concentration p_0^2 (instead of the product of net doping and total boron concentration $p_0 \times N_A$).

Defect annihilation in compensated *n*-type Cz-Si is found to follow a stretched exponential rather than a simple exponential function. The stretching factor increases with increasing net doping concentration n_0, while the annihilation rate R_{ann} decreases with increasing n_0.

II. EXPERIMENTAL DETAILS

In this work, we use samples from two compensated Cz-Si ingots, which were doped with both boron and phosphorus. In Ingot A, the boron and phosphorus concentrations added to the melt were $[B]_{melt}=[P]_{melt}=3\times10^{16}$ cm^{-3}. As a result, the transition from *p*- to *n*-type conductivity is located at about 98% relative distance from the seed end. The interstitial oxygen concentration $[O_i]$, as determined via Fourier transform infrared spectroscopy, decreases with increasing

a)Electronic mail: lim@isfh.de.

distance from the seed end, from $[O_i]=(10\pm2)\times10^{17}$ cm^{-3} to $[O_i]=(7\pm1)\times10^{17}$ cm^{-3}. In ingot B, the boron concentration added to the melt was $[B]_{melt}=6\times10^{16}$ cm^{-3} while the phosphorus concentration added to the melt was $[P]_{melt}=9\times10^{16}$ cm^{-3}. The transition from *p*- to *n*-type conductivity is located at about 25% ingot height. The interstitial oxygen concentration $[O_i]$ decreases from $[O_i]=(11\pm3)\times10^{17}$ cm^{-3} to $[O_i]=(7\pm1)\times10^{17}$ cm^{-3} with increasing distance from the seed end. The resistivity of the *p*-type samples from ingot A ranges from 1.4 to 5.1 Ω cm while the *n*-type wafers from Ingot B have resistivities between 0.29 and 4.9 Ω cm.

For lifetime measurements, the samples were damage-etched and RCA-cleaned. Subsequently, the samples underwent a phosphorus diffusion (50 min at 847 °C) to remove any fast-diffusing metal impurities. The resulting n^+-layers on both sides were removed by a short etch in KOH before passivation by plasma-enhanced chemical vapor-deposited silicon nitride.[9]

Lifetime measurements were performed at 29 °C using the quasi-steady-state photoconductance decay technique (QSSPC).[10] The carrier lifetime τ was extracted at a fixed injection level of $\Delta n=0.1\times n_0$ (or p_0), if not stated otherwise. Note that the determination of the excess carrier density via conductance measurements is sensitive to changes in the mobility, which in turn has already been found to be reduced in boron- and phosphorus-doped compensated Cz-Si.[11,12] We thus determined both the majority- and minority-carrier low-injection mobilities in all samples and used the extracted data in the analysis of the lifetime measurements, noting that low-injection mobilities are appropriate for the injection level at which the carrier lifetimes are reported.

The majority-carrier mobility μ_{maj} was obtained from a combination of four-point-probe (4-pp) resistivity ρ measurements and the determination of the net doping concentration n_0 (or p_0) with the electrochemical capacitance voltage (ECV) method[13,14] according to $\mu_e=(n_0\times\rho\times q)^{-1}$ and $\mu_h=(p_0\times\rho\times q)^{-1}$, respectively ($q$ is the elementary charge). We estimate a 10% uncertainty for the ECV measurements, which results in a 10% uncertainty of the majority-carrier mobility. When applied to noncompensated control samples, this method results in $\mu_h=(480\pm50)$ cm^2/V s in 1.3 Ω cm *p*-type and $\mu_e=(1750\pm200)$ cm^2/V s in 1.5 Ω cm *n*-type silicon. These values are slightly higher than those derived from standard mobility models. For example, in the model of Klaassen,[15,16] $\mu_h=432$ cm^2/V s in noncompensated 1.3 Ω cm *p*-type silicon, whereas $\mu_e=1320$ cm^2/V s in noncompensated 1.5 Ω cm *n*-type silicon. However, the agreement between our measurements and the theoretical values is still good.

The minority-carrier mobility μ_{min} was obtained from effective carrier lifetime τ_{eff} measurements on as-cut wafers using the microwave-detected photoconductance decay (MW-PCD) technique. Due to the saw damage, the surface recombination velocity S of these samples is extremely high ($>10^6$ cm/s). As a result, the effective lifetime τ_{eff} is dominated by the diffusion of carriers to the surfaces. By keeping the sample in low-injection, i.e. $\Delta p \ll n_0$, minority-carrier diffusion becomes the limiting factor and the minority-carrier diffusion coefficient D_{min} can be extracted via

$$\frac{1}{\tau_{eff}}=\frac{1}{\tau_b}+\left(\frac{\pi}{W}\right)^2 D_{min}, \quad (1)$$

where τ_b is the bulk lifetime and W is the sample thickness.[17] Measurements on noncompensated samples yielded $\mu_e=(1180\pm40)$ cm^2/V s in 1.0 Ω cm *p*-type and $\mu_h=(424\pm20)$ cm^2/V s in 1.0 Ω cm *n*-type FZ-Si (compared to $\mu_e=1060$ cm^2/V s and $\mu_h=440$ cm^2/V s according to Klaassen's mobility model[15,16]). Note that we assumed an infinite bulk lifetime in the analysis. Given that effective lifetimes down to 20 μs were measured in degraded *p*-type silicon samples, this assumption may result in an overestimation of the minority-carrier mobility by up to 20%. However, we would like to emphasize that this assumption will always result in an overestimation of the minority-carrier mobility. As a result, a measured reduction in μ_{min} cannot be attributed to this simplification.

In order to generate the boron–oxygen-related recombination centers, the samples were placed under a halogen lamp of 10 mW/cm^2 light intensity. The sample temperature under illumination was 30 °C. The defect annihilation was performed on a hot-plate which was set at 200 °C. In equilibrium, the sample temperature on the hot-plate was (200 ± 2) °C, as measured with a fixed thermocouple. However, for each lifetime measurement the samples are removed from the hot-plate and subsequently returned. When the sample is placed on the hot-plate again, heating to 200 °C takes 20 to 30 s. If the studied time interval at 200 °C in the dark is of the same order, the impact of this delay is obviously not negligible. In the present study, this applies to the first (accumulated) five minutes of measurement time.

In compensated silicon, the absolute dopant concentrations, i.e. N_A and N_D, are also of great importance. It has been shown that, in the presence of interstitial iron Fe_i, it is possible to determine the boron concentration N_A in compensated *p*-type silicon via the iron-acceptor association time constant τ_{assoc}.[18] The phosphorus concentration N_D then follows from $N_D=N_A-p_0$. However, no such easy technique has so far been developed for *n*-type silicon.

Since all *n*-type wafers in the present study were cut from the same ingot, however, at least the trend of the total boron N_A and phosphorus N_D concentrations is known: due to segregation, N_A and N_D increase with increasing distance from the seed end. Accordingly, N_A and N_D increase with increasing net doping concentration n_0.

III. RESULTS AND DISCUSSION

Table I summarizes the mobility data obtained for the studied *p*-type Cz-Si wafers from Ingot A. The hole mobility μ_h follows from a combination of 4-pp resistivity ρ measurements and the determination of the equilibrium hole concentration p_0 using the ECV technique. The electron mobility μ_e was obtained from spatially-resolved effective carrier lifetime τ_{eff} measurements on as-cut wafers. The error margins of μ_e stated in the table refer to variations over the wafer

TABLE I. Resistivities ρ of the studied p-type Cz-Si samples as measured by the 4-pp method, equilibrium hole concentrations $p_{0.ECV}$ determined via ECV measurements, hole mobilities $\mu_{h.ECV}$ calculated from ρ and $p_{0.ECV}$, electron mobilities $\mu_{e.MW\text{-}PCD}$ determined from effective lifetime measurements on as-cut wafers, total boron concentrations N_A determined via the iron-acceptor association time constants τ_{assoc}, and total phosphorus concentrations N_D, calculated using N_A and $p_{0.ECV}$.

Relative distance from seed end	ρ from 4-pp (Ω cm)	$p_{0.ECV}$ from ECV (cm^{-3})	$\mu_{h.ECV}$ (cm^2/V s)	$\mu_{e.MW\text{-}PCD}$ (cm^2/V s)	N_A from τ_{assoc} (cm^{-3})	$N_D=N_A-p_0$ (cm^{-3})
0.16	1.45	1.3×10^{16}	326 ± 33	838 ± 32	1.5×10^{16}	0.2×10^{16}
0.32	1.50	1.2×10^{16}	329 ± 33	792 ± 33	1.8×10^{16}	0.6×10^{16}
0.48	1.70	1.1×10^{16}	320 ± 32	789 ± 34	1.9×10^{16}	0.8×10^{16}
0.66	2.1	9.0×10^{15}	323 ± 32	733 ± 34	1.9×10^{16}	1.0×10^{16}
0.82	3.7	6.1×10^{15}	272 ± 27	656 ± 34	2.1×10^{16}	1.5×10^{16}
0.88	5.1	4.5×10^{15}	271 ± 27	593 ± 36	2.3×10^{16}	1.8×10^{16}

area. The total boron concentration N_A was determined through the iron-acceptor association time constant τ_{assoc}.

Table II compares the measured mobilities of the p-type samples with mobilities of noncompensated wafers of the same resistivity according to the model of Klaassen.[15,16] In accordance with previous work,[12] we find a reduction in both majority- and minority-carrier mobility by 25% to 60% when compared to noncompensated Cz-Si of similar resistivity. This reduction can be attributed to increased amounts of ionized impurities, which result in increased scattering of the free charge carriers. Accordingly, the largest reduction (40% to 60%) is observed at the tail end of the ingot, where the dopant concentrations are the highest.

The mobility data obtained of the examined n-type Cz-Si wafers from Ingot B is summarized in Table III. Again we observe a pronounced reduction in both the majority- and the minority-carrier mobility in all samples compared to noncompensated Cz-Si of the same resistivity. In addition, the electron mobility μ_e decreases significantly with increasing resistivity. Note that this reduction cannot be attributed to a significant increase in the number of scattering centers, as was the case for Ingot A, since the transition region from p- to n-type conductivity in Ingot B already occurs at 25% ingot height, where the dopant concentrations are almost constant. Instead the observed reduction can be explained by lack of screening of the ionized impurities: while the sum of donor N_D and acceptor atoms N_A remains almost constant, the free carrier concentration p_0 (and beyond the transition n_0) decreases significantly, resulting in a weakened screening of the ionized impurities and accordingly in increased scattering cross sections.[19] The mobility data from Tables I and III was used in the following analysis of the QSSPC measurements.

Figure 1 depicts the typical time t dependence of the lifetime τ during (a) defect generation (i.e., LID) and (b) defect annihilation in a p- (triangles up) and n-type sample (triangles down) on a double-logarithmic scale. The samples have a similar net doping of $n_0=p_0=1.0\times10^{16}$ cm^{-3}. The defect generation was performed at a light intensity of 10 mW/cm^2 and a temperature of 30 °C while the defect annihilation was performed at 200 °C in the dark. Complete defect generation in both the p- and the n-type sample takes approximately 50 h, however, the shape of the reduction in the lifetime over time in the two samples differs considerably. On the other hand, defect annihilation in the n-type sample takes about 1000 times as long as in the p-type sample. This finding is in agreement with a recent publication, where the defect annihilation at 215 °C in the dark was reported to take more than 3.5 h in a compensated n-type Cz-Si sample.[8]

To determine the rate of the defect generation R_{gen}, the lifetime data τ is converted to a normalized defect concentration N_t^*, according to $N_t^*(t)\equiv\tau^{-1}(t)-\tau_0^{-1}$, where t is the duration of illumination and τ_0 is the lifetime after complete defect annihilation. The dependence of N_t^* on t can then be described by an exponential rise to maximum function of the form $N_t^*(t)=N_{t.max}[1-\exp(-R_{gen}t)]$, where $N_{t.max}$ is the final defect concentration.

In exclusively boron-doped Cz-Si, the normalized defect concentration N_t^* was found to increase linearly with the bo-

TABLE II. Resistivities ρ of the studied p-type Cz-Si samples as measured by the 4-pp method, measured hole mobilities $\mu_{h.ECV}$ from Table I, hole mobilities $\mu_{h.K}$ in noncompensated silicon of resistivity ρ according to Klaassen's model, measured electron mobilities $\mu_{e.MW\text{-}PCD}$ from Table I, and electron mobilities $\mu_{h.K}$ in noncompensated silicon of resistivity ρ according to Klaassen's model.

Relative distance from seed end	ρ from 4-pp (Ω cm)	$\mu_{h.ECV}$ (cm^2/V s)	$\mu_{h.K}$ (cm^2/V s)	$\mu_{e.MW\text{-}PCD}$ (cm^2/V s)	$\mu_{e.K}$ (cm^2/V s)
0.16	1.45	326 ± 33	435	838 ± 32	1118
0.32	1.50	329 ± 33	436	792 ± 33	1123
0.48	1.70	320 ± 32	440	789 ± 34	1145
0.66	2.1	323 ± 32	445	733 ± 34	1176
0.82	3.7	272 ± 27	456	656 ± 34	1248
0.88	5.1	271 ± 27	460	593 ± 36	1280

TABLE III. Resistivities ρ of the studied n-type Cz-Si samples as measured by the 4-pp method, equilibrium electron concentrations $n_{0.ECV}$ determined via ECV measurements, electron mobilities $\mu_{e.ECV}$ calculated from ρ and $n_{0.ECV}$, electron mobilities $\mu_{e.K}$ in noncompensated silicon of resistivity ρ according to Klaassen's model, hole mobilities $\mu_{h.MW\text{-}PCD}$ determined from effective lifetime measurements on as-cut wafers, and hole mobilities $\mu_{h.K}$ in noncompensated silicon of resistivity ρ according to Klaassen's model.

Relative distance from seed end	ρ from 4-pp (Ω cm)	$n_{0.ECV}$ from ECV (cm^{-3})	$\mu_{e.ECV}$ (cm^2/V s)	$\mu_{e.K}$ (cm^2/V s)	$\mu_{h.MW\text{-}PCD}$ (cm^2/V s)	$\mu_{h.K}$ (cm^2/V s)
0.37	4.9	5.6×10^{15}	285 ± 28	1385	201 ± 16	464
0.49	1.9	6.8×10^{15}	500 ± 50	1336	221 ± 13	453
0.62	1.05	1.0×10^{16}	595 ± 60	1290	237 ± 14	442
0.74	0.65	1.4×10^{16}	683 ± 69	1228	241 ± 11	428
0.88	0.43	2.0×10^{16}	747 ± 75	1185	252 ± 11	418
0.99	0.29	2.9×10^{16}	746 ± 75	1086	243 ± 17	396

ron concentration N_A.[2,4–6] This finding has been explained by a defect model where the recombination center is composed of a substitutional boron atom B_s and an interstitial oxygen dimer O_{2i} to form a recombination-active B_sO_{2i} complex.[4,20,21] In a recent study on B- and P-doped compensated p-type Cz-Si, however, Kopecek *et al.*[22] presented results which suggested that N_t^* actually depends on p_0 and not on N_A. Even more recently, we presented similar findings, however, the data base in this study was quite small (only two data points).[23] To verify these recent findings on a wider data base, Fig. 2 shows the normalized defect concentration N_t^* measured in the compensated p-type samples from Ingot A plotted versus both p_0 (triangles up) and N_A (triangles down).

Conveniently, the net doping concentration p_0 and the total boron concentration N_A in our Ingot A exhibit opposing trends: p_0 decreases with increasing distance from the seed end, while N_A increases with increasing distance from the seed end. As a result, we observe an increase in N_t^* with increasing p_0 but a decrease in N_t^* with increasing N_A. However, it should be noted that (in noncompensated p-type Cz-Si) the defect concentration N_t^* has also been found to depend quadratically on the interstitial oxygen concentration $[O_i]$.[2,4–6]

In the present set of samples, $[O_i]$ decreases with increasing distance from the seed end of the ingot and accordingly with increasing N_A. As a result, one might expect an increase in N_t^* due to the increase in N_A and simultaneously a decrease in N_t^* due to the decrease in $[O_i]$. The interstitial oxygen concentration in ingot A decreases from $[O_i]=(10\pm2)\times10^{17}$ cm^{-3} to $[O_i]=(7\pm1)\times10^{17}$ cm^{-3}. This decrease accounts for a decrease of N_t^* by a factor of 2. However, we observe a decrease in the defect concentration by a factor of 3. Given that the decrease in N_t^* due to the decrease in $[O_i]$ would also be counteracted by the increase due to the increasing boron concentration N_A, the observed decrease cannot be fully attributed to this effect.

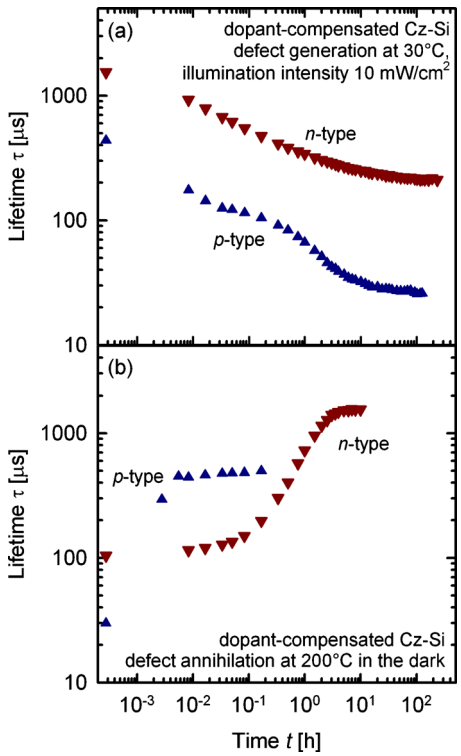

FIG. 1. (Color online) Typical time dependence of the carrier lifetime τ in compensated p- and n-type Cz-Si under (a) 10 mW/cm^2 illumination at 30 °C and (b) at 200 °C in the dark.

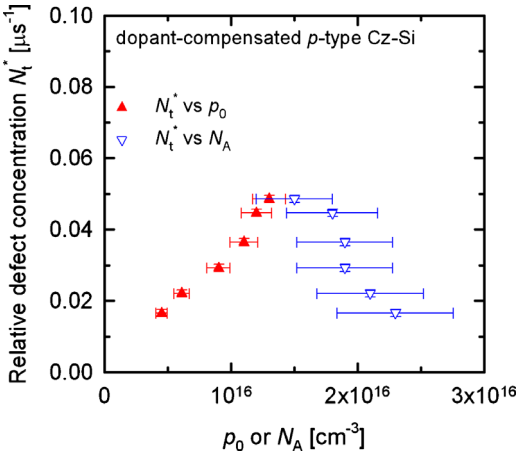

FIG. 2. (Color online) Normalized defect concentration N_t^* in dopant-compensated p-type Cz-Si plotted vs the net doping concentration p_0 (triangles up) and the total boron concentration N_A (triangles down). We observe an increase in N_t^* with increasing p_0 but a decrease in N_t^* with increasing N_A. Given that in exclusively B-doped Cz-Si, N_t^* was found to increase with $p_0=N_A$, a decrease in N_t^* with increasing N_A in compensated Cz-Si is highly unlikely. Thus, these results strongly indicate that N_t^* actually depends on p_0 and not on N_A.

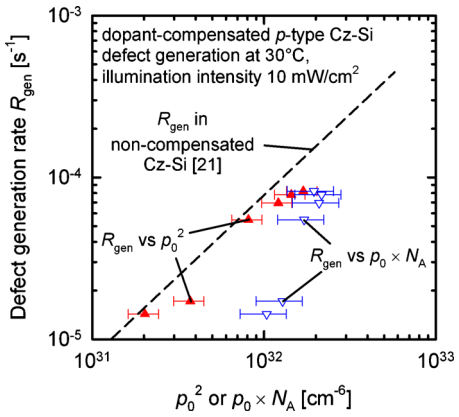

FIG. 3. (Color online) Defect generation R_{gen} determined in dopant-compensated p-type Cz-Si plotted vs the square of net doping concentration p_0^2 (triangles up) and the product of the net doping and the total boron concentration $p_0 \times N_A$ (triangles down). The dashed line is a fit to existing data of R_{gen} in noncompensated Cz-Si, where $p_0 = N_A$.[21] The agreement between compensated and noncompensated material is much better when R_{gen} is plotted vs p_0^2 than for the case where R_{gen} is plotted vs $p_0 \times N_A$.

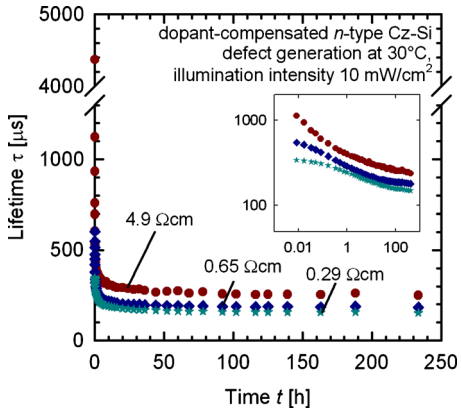

FIG. 4. (Color online) Lifetime τ plotted vs duration of illumination t at 30 °C of three compensated n-type Cz-Si samples with different resistivities ρ (and accordingly different net doping concentrations n_0). To give a better impression of the early stages of LID, the inset shows the data plotted on a double-logarithmic scale.

Given that in all studies on exclusively B-doped Cz-Si an increase in N_t^* with increasing $N_A = p_0$ was observed, an opposing trend in compensated Cz-Si is difficult to explain. On the other hand, an increase in N_t^* with increasing p_0 is in excellent agreement with previous experimental data on both compensated and noncompensated Cz-Si. However, these findings do call for a reassessment of the B_sO_{2i} defect model.[4,21]

Figure 3 depicts the measured values of R_{gen} for the p-type Cz-Si samples as a function of the square of the net doping p_0^2 (triangles up) and as a function of the product of net doping and total boron concentration $p_0 \times N_A$ (triangles down), respectively, on a double-logarithmic scale. We plot R_{gen} versus p_0^2 as well as $p_0 \times N_A$ because in the B_sO_{2i} defect model the defect generation rate R_{gen} depends on $p_0 \times N_A$ [which, in noncompensated Cz-Si, equals $p_0^2 = N_A^2$ and agrees with experimental data on noncompensated B-doped p-type Cz-Si (Refs. 3, 6, and 24)]. However, our recent measurements on two compensated Cz-Si samples suggested that the defect generation rate R_{gen} in compensated p-type Cz-Si actually scales with p_0^2 rather than with $p_0 \times N_A$.[23] With regard to this question, Fig. 3 shows both dependencies.

Figure 3 also depicts a fit to existing experimental data of R_{gen} in noncompensated p-type Cz-Si (dashed line).[21] As can be seen from Fig. 3, the present data is in good agreement with this fit when R_{gen} is plotted versus p_0^2, while we observe considerable deviation if R_{gen} is plotted versus $p_0 \times N_A$. Note that the deviation decreases with increasing $p_0 \times N_A$. This is because in the present set of samples $p_0 \times N_A$ and p_0^2 converge for increasing p_0. This supports recent findings that the defect generation rate in p-type Cz-Si actually depends on p_0^2 rather than on $p_0 \times N_A$.[23] We will discuss the consequences of our experimental results concerning the defect model in more detail in Sec. IV.

Figure 4 shows the evolution of the lifetime τ over time t in three compensated n-type samples with resistivities of 4.9 Ω cm (circles), 0.65 Ω cm (diamonds), and 0.29 Ω cm (stars), respectively. For a better impression of the early stages of degradation, the same data is plotted as an inset on a double-logarithmic scale.

The time dependence of the lifetime τ in compensated n-type samples during defect annihilation at 200 °C in the dark is shown in Fig. 5. The resistivities are 4.9 Ω cm (circles), 1.05 Ω cm (triangles down), and 0.29 Ω cm (stars), respectively. Note that the annihilation takes up to 43000 s (i.e., 12 h), whereas in p-type silicon defect annihilation at 200 °C is complete after 30 s (see Fig. 1). In addition, we find that the lifetime in compensated n-type Cz-Si after defect annihilation is still considerably lower than in exclusively P-doped n-type Cz-Si of similar net doping concentration. For example, the 4.9 Ω cm sample recovers to $\tau = 4.5$ ms, whereas a noncompensated 4.5 Ω cm control sample (with similar passivation) has a lifetime of 12 ms.

Figure 6 shows the normalized defect concentration N_t^* derived from the lifetime data shown in Fig. 5, plotted versus time t at 200 °C in the dark on a double-logarithmic scale. To determine the annihilation rate R_{ann}, we fit a stretched exponential function of the form $y = \exp[-(R_{ann}t)^{\beta}]$ to the experimental data (solid lines).

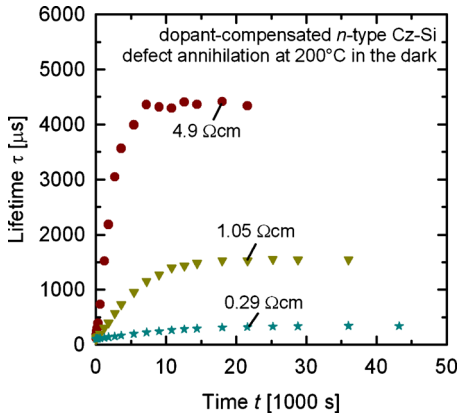

FIG. 5. (Color online) Lifetime τ plotted vs time t at 200 °C in darkness of three compensated n-type Cz-Si samples with different resistivities. The lifetime after complete defect annihilation increases with increasing resistivity.

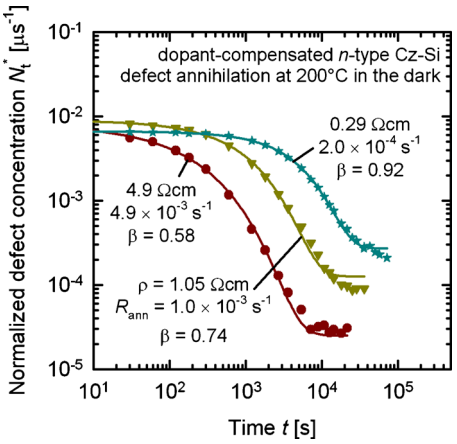

FIG. 6. (Color online) Normalized defect concentration N_t^* derived from the lifetime data shown in Fig. 5, plotted vs time t at 200 °C in the dark on a double-logarithmic scale. In order to determine the defect annihilation rate R_{ann}, a stretched exponential function of the form $y=\exp[-(R_{ann}t)^{\beta}]$ was fitted to the data.

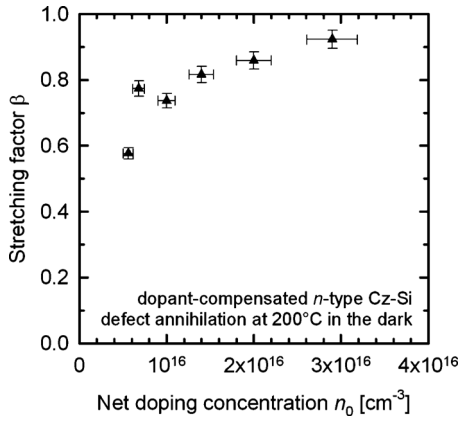

FIG. 8. Stretching factor β obtained from the fits of the defect annihilation rate R_{ann} in compensated n-type Cz-Si (see Fig. 6) plotted vs the net doping concentration n_0. β increases with increasing n_0, approaching 1. A stretching factor β of 1 corresponds to a single exponential decay function, which describes the defect annihilation behavior in B-doped p-type Cz-Si.

The obtained values of R_{ann} are plotted versus the net doping concentration n_0 in Fig. 7 on a double-logarithmic scale. We find a decrease in R_{ann} with increasing n_0, which can be fitted by a power law $R_{ann} \sim n_0^{-1.85}$. Given that the recombination center is boron–oxygen-related, the total boron concentration N_A might also have an impact on R_{ann}. Unfortunately, up to now, no simple method to determine N_A and N_D in compensated n-type silicon has been developed. However, we do know that the boron concentration slowly increases along the ingot height. Accordingly, in the present case, R_{ann} decreases with increasing boron concentration.

Figure 8 shows the stretching factor β (from the fits from Fig. 6) plotted versus the net doping concentration n_0. The stretching factor decreases with decreasing net doping concentration, from $\beta=0.92$ for $n_0=2.9\times10^{16}$ cm^{-3} to $\beta=0.58$ for $n_0=5.6\times10^{15}$ cm^{-3}. Looking at other characteristics of compensated silicon, β also decreases with decreasing total boron concentration N_A and decreasing total phosphorus concentration N_D. On the other hand, β decreases with increasing compensation ratio $R_C \equiv |(N_A+N_D)/(N_A-N_D)|$.

Figure 9 depicts the lifetime τ of a boron-doped oxygen-rich float-zone (O-FZ) wafer plotted versus the excess carrier density Δn, both after complete defect generation (open symbols, "degraded") and complete defect annihilation (filled symbols, "annealed"). Note that the boron concentration in the sample was $N_A=6.8\times10^{14}$ cm^{-3}. As a result, the wafer could be switched from p- to n-type conductivity through the formation of thermal donors. Importantly, LID was observed in both cases.[7] For n-type conductivity, the resistivity was 6 Ω cm, which corresponds to a net doping concentration of $n_0=7.6\times10^{14}$ cm^{-3}.

As can be seen from Fig. 9, there is a strong dependence of the lifetime on the injection level for p-type conductivity (triangles up), whereas the lifetime for n-type conductivity (triangles down) is almost constant over a wide range of Δn. This difference in injection-dependence is a result of the asymmetrical capture-cross sections for electrons σ_n and holes σ_p ($\sigma_n/\sigma_p=10$) of the boron–oxygen-related recombination center.[25]

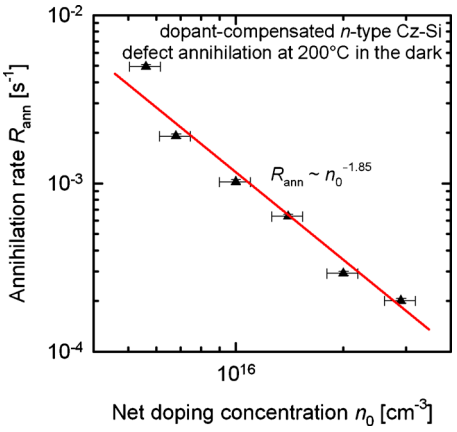

FIG. 7. (Color online) Annihilation rate R_{ann} of compensated n-type Cz-Si samples plotted vs the net doping concentration n_0 on a double-logarithmic scale. The decrease in R_{ann} with increasing n_0 can be described by a power law of the form $R_{ann} \sim n_0^{-1.85}$.

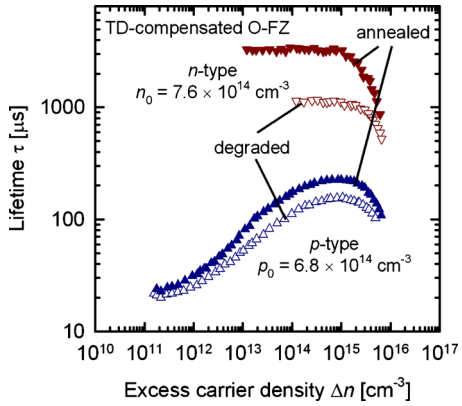

FIG. 9. (Color online) Carrier lifetime τ plotted vs excess carrier density Δn in a boron-doped O-FZ wafer which was switched from p- (triangles up) to n-type conductivity (triangles down) through the formation of thermal donors. LID of the lifetime is observed in both the p- and the n-type state. Due to asymmetrical capture-cross sections for electrons and holes of the boron–oxygen-related recombination center ($\sigma_n/\sigma_p=10$),[25] there is a strong injection-dependence of the lifetime in p-type silicon while the lifetime remains almost constant over a wide range of injection levels in the n-type sample.

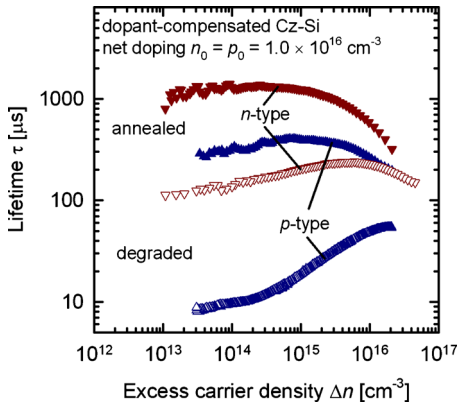

FIG. 10. (Color online) Carrier lifetime τ plotted versus excess carrier density Δn in two boron- and phosphorus-doped compensated Cz-Si wafers, one *p*-type (triangles up) and one *n*-type (triangles down).

Figure 10 shows the lifetime τ plotted versus the excess carrier density Δn in two dopant-compensated samples (i.e., doped with both boron and phosphorus), one *p*- (triangles up) and one *n*-type (triangles down). The samples have a similar net doping concentration of $p_0 = n_0 = 1.0 \times 10^{16}$ cm^{-3}, which is one order of magnitude higher than in the O-FZ samples depicted in Fig. 9. The *n*-type sample in Fig. 10 shows a notably stronger injection-dependence of τ in the degraded state than the *n*-type sample shown in Fig. 9.

In addition, the decrease in the carrier lifetime after LID is much more pronounced for both the *p*- and the *n*-type sample in Fig. 10. For the *p*-type sample, this can be attributed to the higher net doping concentration p_0, which in turn results in a higher defect concentration N_t^*.[22,23] The same might be true for the *n*-type sample. However, the total boron concentration N_A or the injected hole concentration Δp during illumination might also play a role. More detailed work is necessary to clarify this point.

IV. DEFECT MODELS

In noncompensated boron-doped Cz-Si, the defect concentration N_t^* shows a proportional increase with the total boron concentration N_A and a quadratic increase with the interstitial oxygen concentration $[O_i]$.[2,4–6] In addition, the defect generation rate R_{gen} was found to be proportional to N_A^2.[3,6,24] These results led to the development of a defect model where the recombination center is composed of one substitutional boron atom B_s and an interstitial oxygen dimer O_{2i}.[4,20,21] The defect concentration N_t^* is naturally proportional to N_A in this model. Additionally, the defect kinetics of the B_sO_{2i} model predict a proportionality of R_{gen} on the product of the hole concentration and the total boron concentration $p_0 \times N_A$. The dependence on p_0 follows from the requirement of the oxygen dimer to catch a hole to speed up the O_{2i} diffusivity while the dependence on N_A is a consequence of the oxygen dimers bonding with a B_s atom.[21] This model was found to be in excellent agreement with the experimental data measured on noncompensated *p*-type Cz-Si, since in exclusively B-doped Cz-Si $p_0 \times N_A = N_A^2$.

However, in compensated silicon, where the net doping concentration p_0 differs from the total boron concentration N_A, initial results suggest that N_t^* actually depends on p_0 (and not on N_A) (Refs. 22 and 23) and that R_{gen} actually depends on p_0^2 and not on $p_0 \times N_A$.[23] These findings are confirmed in the present study on the base of a much wider data set. As a result, the B_sO_{2i} model needs to be reassessed.

Very recently, an alternative defect model was proposed by Voronkov and Falster.[26] In this model, the recombination center is comprised of one interstitial boron atom B_i and an interstitial oxygen dimer O_{2i}. The interstitial boron concentration $[B_i]$ in this model is proposed to be proportional to the net doping concentration p_0. This dependence follows from the generation of interstitial boron atoms: during ingot cooling, B_i are created via the kick-out mechanism during the creation of oxygen precipitates. Subsequently, the interstitial boron atoms congregate to large clusters. However, at moderate temperatures, B_i^+ atoms (which are positively charged in *p*-type silicon) can also be released from the neutral clusters after capturing a hole h^+. As a result, there is a constant exchange between the two states:

$$B_i^+(\text{dissolved}) \leftrightarrow B_i(\text{cluster}) + h^+.$$

Consequently, the concentration of (dissolved) interstitial boron atoms $[B_i^+]$ is proportional to the hole concentration $[h^+]$, which in turn equals the net doping concentration p_0 (after the ingot temperature passes the intrinsic point). At lower temperature, the exchange between dissolved B_i^+ and B_i clusters eventually ceases and $[B_i^+]$ becomes fixed. In the model of Voronkov and Falster, the interstitial boron atoms B_i^+ then bind with other species such as O_i, O_{2i}, and B_s. However, at room temperature, these complexes are all frozen in and the existing B_iO_{2i} complexes are the so-called latent form of the boron–oxygen-related recombination center.

In this model, the defect concentration N_t^* is proportional to the interstitial boron concentration $[B_i^+]$ which in turn is proportional to the net doping concentration p_0. Accordingly, this model is capable of explaining the experimental finding of our recent and present work that in compensated silicon N_t^* is proportional to p_0 (and not to N_A).

In addition, the model of Voronkov and Falster proposes that the latent form of the B_iO_{2i} complex needs to capture two holes in order to transform into the recombination-active form. As a result, the model predicts a quadratic dependence of R_{gen} on p_0^2, which would be in agreement with both the experimental results on exclusively boron-doped *p*-type Cz-Si and our recent and present findings on B- and P-doped *p*-type Cz-Si.

Note however, that the dependence of N_t^* on p_0 (instead of N_A) would also be true for other defect models involving B_i instead of B_s. For example, a combination of the two models also seems conceivable:[27] in this "hybrid" model, the recombination-active complex would be comprised of an interstitial boron atom B_i and an interstitial oxygen dimer O_{2i}, as proposed by Voronkov and Falster. However, B_i and O_{2i} would be initially separated and the defect formation would proceed via the capture of an oxygen dimer at an interstitial boron atom. As a result, N_t^* would be proportional to $[B_i^+]$ and in turn on p_0, while R_{gen} would be proportional to the

product of p_0 (as the dimer again needs a hole to speed up its diffusivity) and $[B_i^+]$, which in turn equals p_0^2.

With regard to compensated *n*-type Cz-Si, the B_sO_{2i} model predicts a linear dependence of N_t^* on N_A, while the predictions of the B_iO_{2i} model are much more complex and not fully developed, yet.[27] However, in the present study, we observe very similar defect concentrations N_t^* in all *n*-type wafers, even though both n_0 and N_A vary at least by a factor of 5 within the set of samples. Obviously, more detailed studies are necessary to fully understand the composition and the formation mechanism of the boron–oxygen-related recombination center.

V. CONCLUSIONS

We have presented time-dependent lifetime measurements during LID and subsequent lifetime recovery at elevated temperature in the dark in compensated *p*- and *n*-type Cz-Si samples doped with both boron and phosphorus. The defect generation has been found to proceed in comparable time intervals in both compensated *p*- and *n*-type Cz-Si. However, in compensated *n*-type Cz-Si, the evolution of the lifetime during defect generation (at constant light intensity and temperature) cannot be described by a simple exponential function (as is the case in B-doped *p*-type Cz-Si). The reaction speed of the defect annihilation has been found to be reduced by up to three orders of magnitude in compensated *n*-type Cz-Si when compared to compensated *p*-type Cz-Si of similar net doping concentration p_0 (and comparable total boron concentration N_A).

In addition, we have determined the normalized defect concentration N_t^* in compensated *p*-type Cz-Si samples of varying net doping concentrations p_0 and total boron concentrations N_A and observed a proportional increase in N_t^* with increasing p_0 (rather than a proportionality between N_t^* and N_A). When compared to data obtained on exclusively B-doped *p*-type Cz-Si, the defect generation rate R_{gen} in compensated *p*-type Cz-Si showed better agreement when R_{gen} was plotted versus p_0^2 than for the case where R_{gen} was plotted versus $p_0 \times N_A$.

As a consequence, similar carrier lifetime limits can be expected in boron-doped compensated *p*-type silicon and in exclusively B-doped Cz-Si of the same net doping concentration. Accordingly, compensation itself is not expected to further limit the performance of solar cells made on compensated *p*-type Cz-Si.

The defect annihilation in compensated *n*-type Cz-Si was observed to exhibit stretched exponential characteristics, where the stretching factor β increased with increasing net doping concentration n_0. Additionally, we found an inverse dependence of the defect annihilation rate R_{ann} on n_0, which could be described by a power law $R_{ann} \sim n_0^{-1.85}$.

The injection-dependent carrier lifetime in B- and P-doped compensated *p*- and *n*-type Cz-Si was studied and compared to data obtained on B-doped O-FZ silicon, which was overcompensated through the formation of thermal donors. We found a stronger injection-dependence of τ in the dopant-compensated *n*-type sample as well as an overall increased reduction in the lifetime due to LID. For the *p*-type case, this reduction can be attributed to a higher density of boron–oxygen-related recombination centers in the sample due to a higher net doping concentration p_0.

In light of the present findings, we have discussed the standard defect model for the boron–oxygen-related recombination center, in which the recombination center is comprised of a substitutional boron atom B_s and an interstitial oxygen dimer O_{2i}, concluding that the experimental results cannot be explained by the B_sO_{2i} model. In addition, we have discussed a recently proposed defect model in which the complex is comprised of an interstitial boron atom B_i and an interstitial oxygen dimer O_{2i}, and concluded that the B_iO_{2i} model is capable of explaining the present experimental results. Still, more experiments are needed to validate the B_iO_{2i} model and in particular the proposed formation kinetics.

ACKNOWLEDGEMENTS

Funding was provided by the State of Lower Saxony. D.M. is supported by an Australian Research Council QEII Fellowship. The authors are grateful to Karl Hesse, Erich Dornberger, and Laszlo Fabry from Wacker Chemie AG for kindly providing the silicon wafers and to Denise Kreßner-Kiel from Technische Universität Bergakademie Freiberg for the FTIR measurements.

[1] J. Schmidt, A. G. Aberle, and R. Hezel, *Proceedings of the 26th IEEE Photovoltaic Specialists Conference*, Anaheim, CA (IEEE, New York, 1997), p. 13.
[2] S. W. Glunz, S. Rein, W. Warta, J. Knobloch, and W. Wettling, *Proceedings of the Second World Conference and Exhibition on Photovoltaic Solar Energy Conversion*, Vienna, Austria (WIP, Munich, 1998), p. 1343.
[3] S. W. Glunz, S. Rein, J. Y. Lee, and W. Warta, J. Appl. Phys. **90**, 2397 (2001).
[4] J. Schmidt and K. Bothe, Phys. Rev. B **69**, 024107 (2004).
[5] K. Bothe, R. Sinton, and J. Schmidt, Prog. Photovoltaics **13**, 287 (2005).
[6] K. Bothe and J. Schmidt, J. Appl. Phys. **99**, 013701 (2006).
[7] K. Bothe, J. Schmidt, and R. Hezel, *Proceedings of the 29th IEEE Photovoltaic Specialists Conference*, New Orleans, LA (IEEE, New York, 2002), p. 194.
[8] T. Schutz-Kuchly, J. Veirman, S. Dubois, and D. R. Heslinga, Appl. Phys. Lett. **96**, 093505 (2010).
[9] T. Lauinger, J. Schmidt, A. G. Aberle, and R. Hezel, Appl. Phys. Lett. **68**, 1232 (1996).
[10] R. Sinton and A. Cuevas, Appl. Phys. Lett. **69**, 2510 (1996).
[11] J. Libal, S. Novaglia, M. Acciarri, S. Binetti, R. Petres, J. Arumughan, R. Kopecek, and A. Prokopenko, J. Appl. Phys. **104**, 104507 (2008).
[12] F. E. Rougieux, D. Macdonald, A. Cuevas, S. Ruffell, J. Schmidt, B. Lim, and A. Knights, J. Appl. Phys. **108**, 013706 (2010).
[13] E. Peiner, A. Schlachetzki, and D. Krüger, J. Electrochem. Soc. **142**, 576 (1995).
[14] R. Bock, P. P. Altermatt, and J. Schmidt, *Proceedings of the 23rd European Photovoltaic Solar Energy Conference*, Valencia, Spain (WIP, Munich, 2008), p. 1510.
[15] D. B. M. Klaassen, Solid-State Electron. **35**, 953 (1992).
[16] D. B. M. Klaassen, Solid-State Electron. **35**, 961 (1992).
[17] A. B. Sproul, M. A. Green, and A. W. Stephens, J. Appl. Phys. **72**, 4161 (1992).
[18] D. Macdonald, A. Cuevas, and L. J. Geerligs, Appl. Phys. Lett. **92**, 202119 (2008).
[19] B. Lim, M. Wolf, and J. Schmidt, "Carrier mobilities in multicrystalline silicon wafers made from UMG-Si," Phys. Status Solidi C (in press).
[20] J. Adey, R. Jones, D. W. Palmer, P. R. Briddon, and S. Öberg, Phys. Rev. Lett. **93**, 055504 (2004).

[21]D. W. Palmer, K. Bothe, and J. Schmidt, Phys. Rev. B **76**, 035210 (2007).
[22]R. Kopecek, J. Arumughan, K. Peter, E. A. Good, J. Libal, M. Acciarri, and S. Binetti, *Proceedings of the 23rd European Photovoltaic Solar Energy Conference*, Valencia, Spain (WIP, Munich, 2008), p. 1855.
[23]D. Macdonald, F. Rougieux, A. Cuevas, B. Lim, J. Schmidt, M. Di Sabatino, and L. J. Geerligs, J. Appl. Phys. **105**, 093704 (2009).
[24]S. Rein, T. Rehrl, W. Warta, S. W. Glunz, and G. Willeke, *Proceedings of the 17th European Photovoltaic Solar Energy Conference*, Munich, Germany (WIP, Munich, 2001), p. 1555.
[25]S. Rein and S. W. Glunz, Appl. Phys. Lett. **82**, 1054 (2003).
[26]V. V. Voronkov and R. Falster, J. Appl. Phys. **107**, 053509 (2010).
[27]D. Macdonald, A. Liu, F. Rougieux, A. Cuevas, B. Lim and J. Schmidt, "The impact of dopant compensation on the boron-oxygen defect in *p*- and *n*-type crystalline silicon," Phys. Status Solidi A (in press).